Ultrasound shear wave elastography for detection of myocardial fibrosis

Peer-reviewed author version

Petrescu, Aniela; Cvijic, Marta; Wouters , Laurine; Youssef, Ahmed; Bezy, Stephanie; Orlowska, Marta; Degtiarova, Ganna; DUCHENNE, Jürgen; Bogaert, Jan; D'hooge, Jan & Voigt, Jens-Uwe (2025) Ultrasound shear wave elastography for detection of myocardial fibrosis. In: European Heart Journal-Cardiovascular Imaging,.

DOI: 10.1093/ehjci/jeaf200
Handle: http://hdl.handle.net/1942/46601

Ultrasound shear wave elastography for detection of myocardial fibrosis

Aniela Petrescu[1)3)], Marta Cvijic[1)4)], Laurine Wouters[1)], Ahmed Youssef[1)5)], Stéphanie Bézy[1)], Marta Orlowska[1)], Ganna Degtiarova[1)], Jürgen Duchenne[1)6)7)], Jan Bogaert[8)9)], Jan D'hooge[1)], Jens-Uwe Voigt,[1)2)]

1) Department of Cardiovascular Sciences, KU Leuven, Leuven, Belgium
2) Department of Cardiovascular Diseases, University Hospitals Leuven, Leuven, Belgium
3) Department of Cardiology, Mainz University Hospital, University of Mainz, Mainz, Germany
4) Department of Cardiology, University Medical Centre Ljubljana, Slovenia
5) Department of Cardiovascular medicine, Suez Canal University, Ismailia, Egypt
6) Research Group Cardiology & Organ Systems, UHasselt, Diepenbeek, Belgium
7) Department of Cardiology, Heart Centre Hasselt, Jessa Hospital, Hasselt, Belgium
8) Department of Radiology, University Hospitals Leuven, Leuven, Belgium
9) Department of Imaging and Pathology, KU Leuven, Leuven, Belgium

Total word count: 6497

Brief title: Shear wave velocities depend on the fibrosis burden

Corresponding author contact information

Prof. Dr. Jens-Uwe Voigt
KU Leuven and University Hospitals Leuven
Herestraat 49, 3000 Leuven, Belgium
Tel.: +32 / 16 / 349016
Email: jens-uwe.voigt@uzleuven.be

There are no conflicts of interest.

ACKNOWLEDGMENTS:

This work was supported by the European Research Council (FP7/2007-2013, ERC/281748) and the Research Foundation Flanders (FWO; G002617N, G092318N). Aniela Petrescu was supported by a German Society of Cardiology Research Grant. Marta Cvijic was supported by a European Association of Cardiovascular Imaging Research Grant. Ahmed Youssef was supported by the Egyptian ministry of research and high education scholarship,

the Belgian Fund for Cardiac surgery and a European Association of Cardiovascular Imaging Research Grant. Jürgen Duchenne was supported by the FWO (12ZZN22N). Jens-Uwe Voigt holds a personal research mandate of the FWO (1832922N).

Key Words: high frame rate echocardiography; shear wave; myocardial stiffness; myocardial fibrosis

STRUCTURED ABSTRACT (248 words)

Background: Diffuse interstitial or replacement fibrosis is a common feature of a large variety of cardiomyopathies. These alterations contribute to increased myocardial stiffness (MS). Echocardiographic shear wave (SW) elastography is an emerging approach for measuring MS *in vivo*. SWs occur after mechanical excitation of the myocardium, e.g. after mitral valve closure (MVC), and their propagation velocity is directly related to MS.

Objectives: To investigate if SW velocities (SWV) can distinguish between interstitial and replacement fibrosis.

Methods and results: 52 patients (30 heart transplanted patients [52.6±16.0 years, 80% male] and 22 hypertrophic cardiomyopathy patients [54.4±15.6 years, 85% male]) and 37 healthy volunteers (47.2±16.6 years, 76% male) were included. SW elastography was performed using an experimental scanner at 1172±302 frames per second. Patients were classified according to T1 mapping, extracellular volume (ECV) mapping and late gadolinium enhancement measured by cardiac magnetic resonance into three groups: no fibrosis (NF), interstitial fibrosis (MIF) and replacement fibrosis (MRF).

SWVs differed among groups ($p<0.001$), with a significant post-hoc test between MIF and MRF and subjects without fibrosis (6.5±1.1 m/s and 8.7±1.2 m/s), respectively. Significant correlations were noted between SWVs and ECV values ($r=0.70$, $p<0.0001$) and native T1 values ($r=0.48$, $p=0.0004$). SWVs below 6.0 m/s showed the highest accuracy to identify patients without fibrosis (sensitivity 90%, specificity 90%, AUC=0.95). A cut-off of 8.1 m/s could distinguish MRF from MIF (sensitivity 69%, specificity 100%, AUC=0.92).

Conclusions: Natural shear wave velocities can distinguish between normal and pathological myocardium and depend on the fibrosis burden of the myocardium.

ABBREVIATIONS LIST

CMR	=	cardiac magnetic resonance
E/E'	=	mitral inflow to mitral relaxation velocity ratio
ED	=	end-diastole
ECM	=	extracellular matrix
ECV	=	extracellular volume
HFR	=	high frame rate
HTx	=	heart transplant
LGE	=	late gadolinium enhancement
LV	=	left ventricle
MIF	=	myocardial interstitial fibrosis
MRF	=	myocardial replacement fibrosis
MS	=	myocardial stiffness
MVC	=	mitral valve closure
SW	=	shear wave
SWI	=	shear wave imaging
SWV	=	shear wave velocity

INTRODUCTION

Myocardial fibrosis represents the key pathway driving ventricular impairment in a large variety of cardiomyopathies. Initially, the regeneration of the extracellular matrix (ECM) is a physiological, protective mechanism after injury healing. Subsequently, the excessive deposition of the ECM leads to pathological remodeling of heart tissue. Based on the progression of fibrosis and its underlying cause, myocardial fibrosis can be divided into two categories: I) myocardial interstitial fibrosis (MIF) that usually occurs earlier in the course of the disease, characterized by an increased ECM deposition without significant loss of cardiomyocytes, and II) myocardial replacement fibrosis (MRF), that is irreversible and occurs following myocyte apoptosis or necrosis. Unlike MRF, MIF is potentially reversible if treatment is started early [1,2]. Thus, it is necessary to reliably identify the underlying stage of the remodeling process in order to enable early introduction of medical therapy targeting fibrosis [3].

Endomyocardial biopsy is the current gold standard for characterizing interstitial changes but it cannot be used routinely due to its invasive nature, is prone to sampling errors, and has limited sensitivity, especially in diffuse or subtle myocardial abnormalities [4]. Alternatively, the most used non-invasive technique is cardiac magnetic resonance (CMR), which can characterize the extent of both MIF and MRF and may have prognostic value in various cardiomyopathies [5]. Late gadolinium enhancement (LGE) detects end-stage, irreversible, replacement fibrosis, whereby it has limitations in assessing and quantitating diffuse, non-focal myocardial injury and fibrosis. T1 mapping allows earlier detection of potentially reversible diffuse fibrosis by quantifying the extracellular volume which increases with increasing ECM deposition, characteristic for MIF. The combination of both methods can distinguish the different types of cardiac fibrosis that can coexist in the diseased heart [6,7]. However, CMR is an expensive diagnostic method that requires considerable skills and resources for image acquisition and analysis, and therefore, not suited as a screening tool in daily practice. In addition, it has limitations in patients with claustrophobia, medical devices or renal insufficiency.

Cardiac shear wave imaging (SWI) using ultrafast ultrasound imaging is an emerging approach that can estimate the stiffness of the myocardium in vivo. The method is based on tracking mechanical shear waves (SW) at ultrafast frame rates. SWs occur after mechanical excitation of the myocardium, either naturally (e.g. after closure of cardiac valves) or artificially induced through direct mechanical excitation or the acoustic radiation force of strong ultrasound pulses[8,9]. The velocity of SWs (*c*) is related to the stiffness of the medium in which they propagate[10] and ranges in normal hearts from 1 to 5 m/s [11], mainly depending on age[12]. Initial studies indicate that SWI is a potential new tool for the noninvasive assessment of myocardial stiffness[13,14].

Myocardial fibrosis contributes to myocardial stiffening and impairs both systolic and diastolic function. Recently, the direct association between the elastography-based MS using the intrinsic velocity propagation of myocardial stretch with histopathological measured myocardial fibrosis showed promising results[15]. Other recent studies have revealed the relation between increased propagation velocity of naturally occurring SW and presence of MIF or MRF detected with CMR[16–18].

Since the presence and type of fibrosis has been shown to have a great clinical relevance as a potentially reversible and dynamic marker of myocardial disease, the aim of the study was to investigate if velocities of natural SWs depend on the fibrosis burden in the myocardium. For the purpose of this study, we analyzed the SW velocity (SWV) at MVC in a heterogenous group of subjects with hypertrophic cardiomyopathy (HCM), heart transplant (HTX) and age-matched healthy volunteers (HV). The selection of the study group was based on previous research that already reported the co-existence of histopathological alterations such as MIF and MRF in these patients' subpopulations.[19–21] In addition to myocyte hypertrophy, myocardial changes in HCM include progressive interstitial alterations characterized by both MIF and MRF[22]. Histological changes accompanying allograft dysfunction also include myocyte hypertrophy and more commonly MIF that tend to progress into MRF [23–25].

METHODS

Study population

93 patients [52 patients after heart transplant (HTX) and 41 patients with established hypertrophic cardiomyopathy (HCM)] referred for routine follow-up to the Department of Cardiovascular Diseases of the University Hospital Gasthuisberg, Leuven between May 2018 and February 2019 were screened to be enrolled in the study. Of these, 52 patients (30 patients after HTX and 22 patients with HCM) with recent CMR and without evidence for acute cardiac events between the time point of CMR and the study examinations, were included in the final analysis. Exclusion criteria comprised ventricular pacing, left bundle branch block, atrioventricular block more than first degree, histological or clinical evidence of allograft rejection, significant left coronary artery stenosis, more than moderate valvular disease, storage disease and poor echogenicity. All patients underwent clinical explorations, electrocardiogram, standard echocardiography, cardiac SW imaging and CMR.

Further, 37 age-matched healthy volunteers (HV; age between 20 to 80 years) recruited between January 2018 and December 2018 were included in the control group. Exclusion criteria were history of heart disease, systolic blood pressure (SBP) > 140 mmHg, diastolic blood pressure (DBP) > 90 mmHg, cardiac arrhythmia, more than mild valvular disease, reduced LV systolic function (EF less than 50%) and poor echocardiographic window. All HV underwent clinical explorations, electrocardiogram, standard echocardiography and cardiac SW imaging.

The study protocol was approved by the Ethic Committee of the University Hospital Leuven and written informed consent was obtained from all participants before inclusion.

Standard Echocardiography

Echocardiographic examinations were performed on a Vivid E9 system (GE Vingmed Ultrasound, Horten, Norway). Data were analysed offline from stored raw data images using EchoPAC PC software (Version 202, GE Vingmed Ultrasound, Horten, Norway). The routine parameters comprised left heart volumes and ejection fraction, assessed with the biplane Simpson method [26], mitral inflow E/A ratio, deceleration time, isovolumetric relaxation time, tissue Doppler E/E' ratio, and an estimate of systolic pulmonary artery pressure as the peak gradient of tricuspid regurgitation [27]. LV global and longitudinal strain was performed using Speckle Tracking.

Shear Wave Imaging

SW imaging was performed in parasternal long axis view of the LV using a custom-made experimental scanner (HD-PULSE), equipped with a clinical phased array transducer (Samsung Medison P2-5AC) at 1172±302 frames per second.

This modality has already been validated in phantoms and described in our previous works [11,28]. Data reconstruction and post-processing was performed using an in-house software (SPEQLE, version 4.6.8, KU Leuven) developed in Matlab (MathWorks Inc., Natick, Massachusetts, USA). Tissue acceleration was calculated from the tissue Doppler velocity estimates from the high frame rate (HFR) data. Anatomical M-modes were extracted along the midline of the LV septum and displayed color coded for acceleration. Valve closure timings were first determined using pulsed-wave Doppler of the mitral inflow, with end-diastole (ED) marked by the end of the A wave [29]. HFR and regular echo recordings were time-aligned using the R wave of the ECG signal. When image quality of the HFR B mode acquisition allowed, visual appreciation of leaflet closure was used to validate mitral valve closure (MVC) timings. SWs, visible as tilted color bands on M-mode images, were identified after MVC and their slopes were measured semi-automatically (Figure 1).

SWV were typically assessed at the basal and mid-ventricular segments of the left ventricle, since these segments are most accessible through the parasternal long-axis view. Data were analyzed by two independent observers (A.P., M.C.), both blinded to any clinical information. All SWV measurements were repeated three times, and the average was used for statistical analysis.

Cardiac magnetic resonance

CMR was performed on a clinical 1.5-Tesla scanner (Ingenia; Philips Healthcare, Germany) by using commercially available CMR imaging software, electrocardiographic triggering, and a cardiac-dedicated phase array coil. The protocol started with Steady-state free-precession breath-hold cine images that were acquired in the vertical and horizontal long-axis, short axis and left ventricular outflow tract view. In order to assess MRF, 3-dimensional phase-sensitive inversion recovery gradient (PSIR) gradient-echo sequences for late-enhancement were performed in all available slices after gadobutrol administration, as previously described in detail[30]. To evaluate the degree of MIF, native T1 mapping was performed using a modified Look-Locker inversion recovery sequence before gadobutrol application on three short-axis slices (basal, mid and apical). For each short-axis image, a region of interest was drawn in the anteroseptal wall to calculate myocardial T1 time as average of basal and mid slices – that corresponded to the area analyzed with shear wave elastography - being careful to exclude the blood pool as well as the epicardial fat **(Figure 1)**. Postcontrast T1 was obtained 15 minutes after gadobutrol application in all available slices, and ECV was derived as previously described [31]. Since prolonged T2 relaxation has been related to transplant edema and possibly rejection, T2 mapping sequences were assessed in mid-ventricular short-axis slices in order to exclude patients with acute events [32]. All images were interpreted by an experienced reader blinded to any other data of the patients.

Normal native myocardial T1 values depend on several technical and physiological parameters[33]. Therefore, MIF was defined in our center as T1 values > 1040 ms and/or ECV>30% without evidence of positive LGE. The presence of LGE in the anteroseptal wall was associated with MRF. According to the

presence and type of fibrosis in the anteroseptal wall, patients were divided into three groups: no fibrosis (NF), MIF and MRF. CMR data were not available in the HV group.

Statistical analysis

Data for continuous variables are presented as means ± standard deviation if normally distributed, or as median and interquartile range if non-normally distributed. Categorical variables are presented as frequencies and percentages. Comparison between groups were made using chi-square tests for categorical variables. Continuous variables were compared with unpaired Student t test or the nonparametric Mann-Whitney U test where appropriate. The association of variables was expressed using Pearson's correlation coefficient. When comparing more than two groups, continuous normally distributed variables were tested using one-way analysis of variance (ANOVA); when F test was significant at the 0.05 level, pairwise comparisons were performed, which were adjusted by using Bonferroni method to correct for multiple comparisons. Multiple linear regression analysis, using the backwards method, was performed to identify the potential variables that were associated with ECV as the best parameter to assess myocardial fibrosis non-invasively. Variables selected in the univariate analysis ($p<0.05$) and those considered clinically important were entered into multivariate analysis. Receiver-operating characteristics (ROC) curves and area under the curve (AUC) were computed to assess optimal cut-off value for the SW velocities to differentiate between subgroups of patients.

Inter-observer variability was evaluated in 30 patients (10 patients from each group, HCM, HTX and HV, respectively) using intra-class correlation coefficient (two-way mixed model, absolute agreement between single measures). A two-sided P value of 0.05 was considered statistically significant for all tests. All statistical analyses were performed using Medcalc (Medcalc Software, Mariakerke, Belgium) and SPSS Statistics Software (Version 29.0.1.0).

RESULTS

Patient characteristics and CMR results

52 patients (30 patients after HTX [52.6±16.0 years, 80% male] and 22 patients with established HCM [54.4±15.6 years, 85% male]) and 37 HV (47.2±16.6 years, 76% male) were included in the final analysis. The time between CMR and echo was a median of 6 months (interquartile range 0 to 12 months). 8 patients with either no evidence of fibrosis or evidence of MRF by positive LGE in a series of CMRs that were conducted at least 1 year both before and after echocardiography were included in the data analysis without repeating the CMR based on their clinical and paraclinical stability.

LGE of non-ischemic pattern in the anteroseptal wall as evidence of MRF was observed in 16 patients (30%), both in HTX (n=2) and HCM (n=14) groups. The native T1 time in the anteroseptal wall could be assessed in all patients, and ECV was calculated in 46 (85%) patients after gadolinium injection. There was evidence of MIF in 15 patients (29%), predominantly in the HTx group (n=12), and 3 patients in the HCM group. According to the presence and type of fibrosis assessed with CMR in the anteroseptal wall, patients were divided into three groups: NF, MIF and MRF **(Figure 1).** Population characteristics including clinical data, echocardiography and CMR measurements were compared between the groups and are reported in **Table 1**.

Diffuse vs. replacement fibrosis

SWVs differed significantly among groups (HV vs. NF vs. MIF vs. MRF; p<0.001), with a significant post-hoc test between NF vs. MIF vs. MRF (4.3±1.3 m/s vs. 6.5±1.1 m/s vs. 8.7±1.2 m/s, respectively; **s. Table 1**). The NF group showed a tendency towards higher SWV than HV, but the difference didn't reach the pre-defined significance level (3.4±1.0 m/s vs. 4.3±1.3 m/s, p=0.06; **Figure 2**).

We found a cut-off value of SWV of 4.6 m/s to distinguish best between HV and all patient groups (sensitivity 73%, specificity 94%, AUV 0.88). SWVs below a cut-off of 6.0 m/s showed the highest accuracy to identify patients without any type of fibrosis (NF vs. MIF + MRF; sensitivity 90%, specificity 90%, area

under the curve=0.95) (**Figure 3A-B)**. A cut-off of 8.1 m/s could differentiate MRF from MIF with a sensitivity and specificity of 69% and 100%, respectively (area under the curve=0.92) **(Figure 3C)**.

Relationship of shear wave velocities with parameters of myocardial fibrosis, remodeling, diastolic function and clinical characteristics

SWVs showed a good correlation with ECV values (r=0.70, p<0.0001) and a moderate correlation with T1 values (r=0.48, p=0.0004) **(Figure 4A-B**).

Overall, standard echocardiographic measures of LV diastolic function showed moderate to weak correlations with SWVs (E/E': r=0.52, p<0.001, **Figure 4C**; IVRT: r=0.39, p<0.001; DT: r=0.28, p=0.01; TV Vmax: r=0.43, p=0.003). There was no significant correlation between SWV and E/A. There were moderate correlations between SWVs and parameters of LV geometry (IVSD: r=-0.54, p<0.001; LVEDD: r=-0.24, p=0.03), age (r=0.36, p<0.001) and global longitudinal strain (r=0.31; p=0.008). Hemodynamic parameters such as heart rate and blood pressure have shown no significant correlations with SWVs.

Echocardiographic predictors of myocardial fibrosis

Univariate regression analysis revealed significant associations of SWV, IVSD, DT and IVRT with ECV – as the gold standard non-invasive parameter for the assessment of myocardial fibrosis **(s. Table 2).** When performing a multiple linear regression model, SWV remained the only predictor of ECV (r=0.73).

Feasibility and Reproducibility of myocardial SW velocity measurements

Myocardial SWs starting immediately after MVC and propagating from the LV base to the apex were detected in 83 subjects (93%). Analysis of the inter-observer variability showed a good reproducibility by using intraclass correlation (intraclass correlation coefficients 0.96; 95% CI, 0.90-0.98 and 0.97, and 98%; CI, 0.95-0.99, respectively).

DISCUSSION

The main finding of the present study was the ability of SWV after MVC to differentiate between

fibrosis and healthy tissue. Secondly, SWV was shown to depend on the content of fibrosis in the myocardium, being able to distinguish between interstitial and replacement fibrosis.

Shear wave imaging can identify variations in local stiffness

The type and amount of cardiac fibrosis has important clinical and prognostic implications, being associated with a long-term risk of death or major adverse cardiac events [20] (34). SWI can detect localized variations in tissue stiffness inside the myocardium that occur as a result of fibrosis [16,34]. Villemain et al. showed a strong relation between the SWV induced by acoustic radiation force at end-diastole and native T1 time (r=0.71; p<0.01) and ECV fraction (r=0.45; p=0.03) in 20 HCM patients[35]. A similar correlation between natural SWV after MVC and native T1 was shown in our previous study in HTX recipients (r=0.75; p<0.001)[18]. In the present study we found significant correlations between native myocardial T1 times, ECV and SWVs. We found a cut-off value of SWV of 6.0 m/s (sensitivity 90 %, specificity 90%, area under the curve=0.95) to identify patients with fibrosis (MIF and MRF).

While the mean SWV in the MIF group was 6.5 ±1.1 m/s, a mean of 8.7±1.2 m/s was measured in the MRF group, indicating an increase in SWV with the increase of the density of fibrosis. Similar values were reported by Wouters et al. that measured significantly higher values in patients with left bundle branch block with septal MRF compared with left bundle branch block patients without septal MRF, both during biventricular pacing ON and OFF (4.9 m/s and 5.6 m/s left bundle branch block without septal MRF vs. 8.3 m/s and 7.7 m/s left bundle branch block with septal MRF, respectively)[36].

In our study, the two patient groups (MIF vs. MRF) had similar baseline characteristics (**see Table 1**), except for the ECV and DT, compatible with disarray and replacement fibrosis with deposition of collagen as confirmed by CMR. Between NF and MIF groups, no other parameter was significantly different besides native T1 as a marker of the presence of MIF with, consequently, an increase in SWV. When running a multiple regression, SWV remained the only predictor of ECV, suggesting that this is the best parameter to indicate local variations in tissue stiffness.

Shear wave velocities depend on the degree of myocardial fibrosis

It has been shown in previous research that MS detected with SWI correlates with both MIF and MRF[18,36,37] In the present work we went a step forward, and investigated if SWs after MVC are able to distinguish between these two fibrosis patterns defined with CMR in different pathologies. We included a heterogenous population where these histopathological alterations commonly coexist, as a model to test the capability of the SWI to detect varieties in the structure of the local tissue, from more subtle changes that are potentially reversible to old fibrous scars that tend to develop later and are irreversible. In the present study, SWV was shown to depend on the fibrosis burden of the myocardium being able to distinguish between the two fibrosis groups - MIF and MRF - with a cut-off of 8.1 m/s with a sensitivity of 69% and a specificity of 100% (area under the curve=0.92). Wouters et al. reported a comparable cut-off value of 7.1 m/s that was found to detect septal MRF with a sensitivity of 80% and a specificity of 93%. [36]

Relationship of SW velocity to parameters of myocardial remodeling, cardiac function, and clinical characteristics

Multiple mechanical factors such as aging, chamber hypertrophy, contractility, diastolic function and fibrosis have been shown to directly affect SW velocity and, therefore, MS[38] We included a control group of age-matched HVs and compared it with the NF group and found no significant difference in the SW velocity in the absence of fibrosis or increased filling pressures estimated with echocardiographic parameters. With a cut-off value of 4.6 m/s, SW velocities after MVC could differentiate between normal and pathological myocardium with 73% sensitivity and 94% specificity. These results are supported by previous research in patients with hypertensive heart disease, where a cut-off value of 5 m/s could differentiate patients with concentric hypertrophy from healthy controls[39].

According to Lamb's theory, wall thickness and curvature can influence wave propagation, particularly in thin walls, where SWV may be underestimated (e.g., in pediatric patients) [40]. However,

Youssef et al.[12] showed in a multiple linear regression analysis in healthy volunteers that wall thickness only remained a significant factor in neonates with a wall thickness of less than 4.4 mm, suggesting that for most adult hearts, wall thickness has a minimal effect on SWV. Furthermore, studies investigating the impact of hypertrophy support the notion that myocardial stiffness, rather than wall thickness alone, primarily determines SWV[39,41] In our study, SWV was higher in patients with MRF than in those with MIF and NF, even though wall thickness did not significantly differ between these groups.

Since natural SWs occur at the onset of the isovolumic contraction phase, both afterload and myocardial contractility (reflected by SBP, EF and GLS) may theoretically influence them. However, earlier animal studies by Bezy et al. [42], where contractility has been modulated, did not reveal any significant relation of contractility and shear waves speed after MVC. Consistent with these findings, afterload and contractility-related parameters such as SBP, EF and GLS used in our study were not significantly different between the patient subgroups in our study, suggesting that natural SWVs at MVC are not influenced by myocardial contractility. Parameters of diastolic function such as E/E' were neither significantly different between the patient subgroups, implying that the variation in SWV in the present study was an indicative of a local variation in tissue stiffness by fibrosis, rather than any other factors. Wall thickness as such had only a minor relation to SWV (supplementary Figure).

Supporting these ideas, Naser et al. showed in HCM patients that segmental MS correlated best with the severity of the histologically assessed myocardial fibrosis, and less strongly with wall thickness or segmental longitudinal strain [15]. Cvijic et al. demonstrated that hypertensive patients with concentric hypertrophy and presumably interstitial fibrosis had higher SWVs than patients with concentric remodeling, despite the presence of septal hypertrophy in both groups [39]. Moreover, after normalizing wall stress, patients with concentric hypertrophy still had higher SWVs, confirming that the differences rather reflect intrinsic myocardial properties than differences in wall thickness or filling pressures.

Study limitations

The study limitations are mostly related to the current methodological approach and have been thoroughly discussed before [38,43]. It should be noted that the visualization of natural shear waves (SW) at mitral valve closure (MVC) is only feasible in the interventricular septum and during the isovolumetric contraction phase. Animal experiments and invasive pressure measurements in patients have shown, however, that such measurements still closely related to end-diastolic myocardial properties [42]. Further, the time between CMR and echocardiography was a median of 6 months (interquartile range 0 to 12 months). However, patients included in the final analysis were clinically stable between measurements and showed no evidence for relevant cardiovascular function changes (symptoms of heart failure, hospitalization for cardiac and non-cardiac cause, ECG, noninvasive imaging, lab parameters) between the examinations. Another limitation of the study is that HVs didn't undergo CMR, therefore T1 and ECV couldn't be included in the analysis of SW velocity predictors in the overall population.

CLINICAL PERSPECTIVES

Given that fibrosis may lead to diastolic dysfunction due to increased myocardial stiffness, SWI might aid in its early detection. Nevertheless, since the subtypes of myocardial fibrosis have different pathophysiology, clinical course, and prognosis, there is a need for improving diagnostic tools to enable early, reliable and non-invasive fibrosis detection and quantification, which might improve prognosis and patients' quality of life.

CONCLUSIONS

Shear wave velocities after mitral valve closure can distinguish between normal and pathological myocardium and variate with the fibrosis burden of the myocardium.

The data underlying this article will be shared on reasonable request to the corresponding author.

BIBLIOGRAPHY

1. Bing R, Cavalcante JL, Everett RJ, Clavel MA, Newby DE, Dweck MR. Imaging and Impact of Myocardial Fibrosis in Aortic Stenosis. *JACC: Cardiovascular Imaging*.
2. Gyöngyösi M, Winkler J, Ramos I, Do QT, Firat H, McDonald K, et al. Myocardial fibrosis: biomedical research from bench to bedside. *European Journal of Heart Failure*.
3. Hinderer S, Schenke-Layland K. Cardiac fibrosis – A short review of causes and therapeutic strategies. *Advanced Drug Delivery Reviews*.
4. Cooper LT, Baughman KL, Feldman AM, Frustaci A, Jessup M, Kuhl U, et al. The role of endomyocardial biopsy in the management of cardiovascular disease: A scientific statement from the American Heart Association, the American College of Cardiology, and the European Society of Cardiology. *Circulation*.
5. Nathan M, Ying LC, Pierre C, David B, João L. Assessment of Myocardial Fibrosis with Cardiac Magnetic Resonance. *J Am Coll Cardiol* 2011;**57**:891.
6. Moon JC, Treibel TA, Schelbert EB. T1mapping for diffuse myocardial fibrosis: A key biomarker in cardiac disease? *Journal of the American College of Cardiology* 2013;**62**:1288–1289.
7. Nakamori S, Dohi K, Ishida M, Goto Y, Imanaka-Yoshida K, Omori T, et al. Native T1 Mapping and Extracellular Volume Mapping for the Assessment of Diffuse Myocardial Fibrosis in Dilated Cardiomyopathy. *JACC Cardiovasc Imaging* 2018;**11**:48–59.
8. Vos HJ, Dalen BM van, Heinonen I, Bosch JG, Sorop O, Duncker DJ, Steen AFW van der, Jong N de. Cardiac shear wave velocity detection in the porcine heart. *Ultrasound Med Biol* 2017;**43**:753–764.
9. Couade M, Pernot M, Messas E, Bel A, Ba M, Hagege A, Fink M, Tanter M. In Vivo Quantitative Mapping of Myocardial Stiffening and Transmural Anisotropy During the Cardiac Cycle. *IEEE Trans Med Imaging* 2011;**30**:295–305.
10. Villemain O, Correia M, Mousseaux E, Baranger J, Zarka S, Podetti I, et al. Myocardial Stiffness Evaluation Using Noninvasive Shear Wave Imaging in Healthy and Hypertrophic Cardiomyopathic Adults. *JACC Cardiovasc Imaging* 2018.
11. Santos P, Petrescu A, Pedrosa J, Orlowska M, Komini V, Voigt J-U, D'hooge J. Natural shear wave imaging in the human heart: normal values, feasibility and reproducibility. *IEEE Trans Ultrason Ferroelectr Freq Control* 2018:1–1.
12. Youssef AS, Petrescu A, Salaets T, Bézy S, Wouters L, Orlowska M, et al. Evolution of Natural Myocardial Shear Wave Behavior in Young Hearts: Determinant Factors and Reproducibility Analysis. *J Am Soc Echocardiogr* 2024.
13. Pernot M, Lee WN, Bel A, Mateo P, Couade M, Tanter M, Crozatier B, Messas E. Shear Wave Imaging of Passive Diastolic Myocardial Stiffness: Stunned Versus Infarcted Myocardium. *JACC Cardiovasc Imaging* 2016.
14. Petrescu A, D'hooge J, Voigt JU. Concepts and applications of ultrafast cardiac ultrasound imaging. *Echocardiography* 2021;**38**.

15. Naser JA, Anupraiwan O, Adigun RO, Maleszewski JJ, Pislaru S V., Pellikka PA, Pislaru C. Myocardial Stiffness by Cardiac Elastography in Hypertrophic Cardiomyopathy. *JACC Cardiovasc Imaging* 2021;**14**:2051–2053.
16. Strachinaru M, Bosch JG, Schinkel AFL, Michels M, Feyz L, Jong N de, et al. Local myocardial stiffness variations identified by high frame rate shear wave echocardiography. *Cardiovasc Ultrasound* 2020;**18**.
17. Kvåle KF, Salles S, Lervik LCN, Støylen A, Løvstakken L, Samset E, Torp H. Detection of Tissue Fibrosis using Natural Mechanical Wave Velocity Estimation: Feasibility Study. *Ultrasound Med Biol* 2020;**46**:2481–2492.
18. Petrescu A., Bézy S., Cvijic M., Santos P., Orlowska M., Duchenne J., et al. Shear Wave Elastography Using High-Frame-Rate Imaging in the Follow-Up of Heart Transplantation Recipients. *JACC Cardiovasc Imaging* 2020;**13**:2304–2313.
19. Armstrong AT, Binkley PF, Baker PB, David Myerowitz P, Leier C V. Quantitative Investigation of Cardiomyocyte Hypertrophy and Myocardial Fibrosis Over 6 Years After Cardiac Transplantation. *Journal of the American College of Cardiology*.
20. Hughes A, Okasha O, Farzaneh-Far A, Kazmirczak F, Nijjar PS, Velangi P, et al. Myocardial Fibrosis and Prognosis in Heart Transplant Recipients. *Circ Cardiovasc Imaging* 2019;**12**.
21. Halliday BP, Prasad SK. The Interstitium in the Hypertrophied Heart. *JACC: Cardiovascular Imaging*.
22. Raman B, Ariga R, Spartera M, Sivalokanathan S, Chan K, Dass S, et al. Progression of myocardial fibrosis in hypertrophic cardiomyopathy: Mechanisms and clinical implications. *Eur Heart J Cardiovasc Imaging* 2019;**20**:157–167.
23. Riesenkampff E, Chen CK, Kantor PF, Greenway S, Chaturvedi RR, Yoo S-J, et al. Diffuse Myocardial Fibrosis in Children After Heart Transplantations. *Transplantation* 2015;**99**:2656–2662.
24. Coelho-Filho OR, Shah R, Lavagnoli CFR, Barros JC, Neilan TG, Murthy VL, et al. Myocardial tissue remodeling after orthotopic heart transplantation: a pilot cardiac magnetic resonance study. *The International Journal of Cardiovascular Imaging 2016 34:1* 2016;**34**:15–24.
25. Rowan RA, Billingham ME. Pathologic changes in the long-term transplanted heart: a morphometric study of myocardial hypertrophy, vascularity, and fibrosis. *Hum Pathol* 1990;**21**:767–772.
26. Lang RM, Badano LP, Mor-Avi V, Afilalo J, Armstrong A, Ernande L, et al. Recommendations for Cardiac Chamber Quantification by Echocardiography in Adults: An Update from the American Society of Echocardiography and the European Association of Cardiovascular Imaging. *Journal of the American Society of Echocardiography* 2015;**28**:1-39.e14.
27. Nagueh SF, Smiseth OA, Appleton CP, Byrd BF, Dokainish H, Edvardsen T, et al Recommendations for the Evaluation of Left Ventricular Diastolic Function by Echocardiography: An Update from the American Society of Echocardiography and the European Association of Cardiovascular Imaging. *Journal of the American Society of Echocardiography* 2016;**29**:277–314.
28. Petrescu A, Santos P, Orlowska M, Pedrosa J, Bézy S, Chakraborty B, et al. Velocities of Naturally Occurring Myocardial Shear Waves Increase With Age and in Cardiac Amyloidosis. *JACC Cardiovasc Imaging* 2019.

29. Mada RO, Lysyansky P, Daraban AM, Duchenne J, Voigt J-U. How to Define End-Diastole and End-Systole? *JACC Cardiovasc Imaging* 2015;**8**:148–157.
30. Barreiro-Pérez M, Curione D, Symons R, Claus P, Voigt JU, Bogaert J. Left ventricular global myocardial strain assessment comparing the reproducibility of four commercially available CMR-feature tracking algorithms. *Eur Radiol* 2018;**28**:5137–5147.
31. Jellis CL, Kwon DH. Myocardial T1 mapping: modalities and clinical applications. *Cardiovasc Diagn Ther* 2014;**4**:126–12637.
32. Vermes E, Pantaléon C, Auvet A, Cazeneuve N, Machet MC, Delhommais A, et al. Cardiovascular magnetic resonance in heart transplant patients: Diagnostic value of quantitative tissue markers: T2 mapping and extracellular volume fraction, for acute rejection diagnosis. *Journal of Cardiovascular Magnetic Resonance* 2018;**20**.
33. Perea RJ, Ortiz-Perez JT, Sole M, Cibeira MT, Caralt TM de, Prat-Gonzalez S, et al.T1 mapping: characterisation of myocardial interstitial space. *Insights into Imaging*.
34. Pernot M, Lee W-N, Bel A, Mateo P, Couade M, Tanter M, et al. Shear wave imaging of passive diastolic myocardial stiffness: Stunned versus infarcted myocardium. *JACC Cardiovasc Imaging* 2016;**9**:1023–1030.
35. Villemain O, Correia M, Mousseaux E, Baranger J, Zarka S, Podetti I, et al. Myocardial Stiffness Evaluation Using Noninvasive Shear Wave Imaging in Healthy and Hypertrophic Cardiomyopathic Adults. *JACC Cardiovasc Imaging* 2019;**12**:1135–1145.
36. Wouters L, Duchenne J, Bézy S, Papangelopoulou K, Puvrez A, Klop B, et al. Septal Scar Detection in Patients With Left Bundle Branch Block Using Echocardiographic Shear Wave Elastography. *JACC Cardiovasc Imaging* 2023.
37. Strachinaru M, Bosch JG, Schinkel AFL, Michels M, Feyz L, Jong N de, et al. Local myocardial stiffness variations identified by high frame rate shear wave echocardiography. *Cardiovasc Ultrasound* 2020;**18**.
38. Caenen A, Pernot M, Nightingale KR, Voigt J-U, Vos HJ, Segers P, D'hooge J. Assessing cardiac stiffness using ultrasound shear wave elastography. *Phys Med Biol* 2022;**67**:02TR01.
39. Cvijic M, Bézy S, Petrescu A, Santos P, Orlowska M, Chakraborty B, et al. Interplay of cardiac remodelling and myocardial stiffness in hypertensive heart disease
40. Caenen A, Bézy S, Pernot M, Nightingale KR, Vos HJ, Voigt JU, et al. Ultrasound Shear Wave Elastography in Cardiology. *JACC Cardiovasc Imaging* 2024;**17**:314–329.
41. Strachinaru M, Bosch JG, Gils L van, Dalen BM van, Schinkel AFL, Steen AFW van der, et al. Naturally Occurring Shear Waves in Healthy Volunteers and Hypertrophic Cardiomyopathy Patients. *Ultrasound Med Biol* 2019;**45**:1977–1986.
42. Bézy S, Duchenne J, Orlowska M, Caenen A, Amoni M, Ingelaere S, et al. Impact of Loading and Myocardial Mechanical Properties on Natural Shear Waves: Comparison to Pressure-Volume Loops. *JACC Cardiovasc Imaging* 2022;**15**.
43. Caenen A, Bezy S, Petrescu A, Werner A, Voigt J-U, Dhooge J, Segers P. Transmural Wave Speed Gradient May Distinguish Intrinsic Myocardial Stiffening from Preload-Induced Changes in Operational Stiffness in Shear Wave Elastography. *IEEE Trans Biomed Eng* 2022:1–12.

FIGURE LEGENDS

Figure 1 (Graphical abstract): Assessment of shear wave velocity in three patients with no fibrosis, interstitial fibrosis and replacement fibrosis. The mid left ventricular segment of the anteroseptal wall obtained with late gadolinium enhancement and T1 mapping were side-by-side compared with the acceleration M-mode map of the anteroseptal wall in each patient. Note that shear wave velocities at mitral valve closure (MVC) increase with the type of fibrosis. The shaded region of the electrocardiogram indicates the time interval covered by the M-mode map above. ECG = electrocardiogram; LGE = late gadolinium enhancement; MVC = mitral valve closure, nT1 = native T1; SWI = shear wave imaging; v = velocity of the shear wave.

Figure 2: Shear wave velocities in healthy volunteers (HV) vs. patients with no fibrosis (NF), myocardial interstitial fibrosis (MIF) and myocardial replacement fibrosis (MRF). Data is expressed as mean ± standard deviation. SW = shear wave.

Figure 3: Receiver operating characteristic curves (ROC). (A) ROC curve for prediction of pathology, with optimal cut-off of 4.6m/s to differentiate between patients with increased myocardial stiffness and healthy volunteers (HV). (B) ROC curve for prediction of myocardial fibrosis with optimal cut-off of 6.0 m/s to detect myocardial fibrosis within the patients' group, (C) ROC for prediction of replacement fibrosis with optimal cut-off of 8.1 m/s to distinguish between interstitial (MIF) and replacement fibrosis (MRF).

Figure 4: Correlation of shear wave propagation velocity with parameters of T1 mapping and diastolic function. Correlation between shear wave (SW) velocity propagation and extracellular volume (ECV) (left). Correlation between SW propagation velocity and native T1 (middle). Correlation between shear wave (SW) velocity propagation and E/E'. SW velocities increase with increasing native T1, ECV and E/E' (right).

Note that the markers are colored individually according to the presence and the type of fibrosis. HV = healthy volunteers, NF = no fibrosis, MIF = myocardial interstitial fibrosis, MRF = myocardial replacement fibrosis.

TABLES

Table 1: Patient characteristics according to the presence and type of fibrosis.

	HV (0) (n=37)	NF (1) (n=21)	MIF (2) (n=15)	MRF (3) (n= 16)	P ANOVA 0 vs. 1	P ANOVA 0 vs. 2	P ANOVA 0 vs. 3	P ANOVA 1 vs. 2	P ANOVA 1 vs. 3	P ANOVA 2 vs. 3	P all groups
Clinical characteristics											
Age (years)	47.2±16.8	50.2±16.6	56.7±16.2	54.4±15.2	ns.	ns.	ns.	ns.	ns.	ns.	0.22
Height (cm)	178±11	175±9	175±8	177±8	ns.	ns.	ns.	ns.	ns.	ns.	0.7
Weight (kg)	76±13	79±12	77±15	88±21	1.00	1.00	**0.03**	1.00	0.3	0.18	**0.04**
BMI	23.9±2.7	25.6±4.2	25.1±4.6	27.8±5.0	0.61	1.00	**0.006**	1.00	0.55	0.31	**0.01**
BSA (m2)	1.9±0.2	2.0±0.2	1.9±0.2	2.1±0.3	ns.	ns.	ns.	ns.	ns.	ns.	0.12
SBP (mmHg)	126±16	137±15	139±13	135±16	0.052	0.057	0.39	1.00	1.00	1.00	**0.01**
DBP (mmHg)	70±11	86.0±10	82±10	78±11	**<0.001**	**0.006**	0.06	1.00	0.17	1.00	**<0.001**
HR (bpm)	63±13	77±11	72±13	68±12	**<0.001**	0.28	1.00	1.00	0.21	1.00	**0.002**
Echocardiographic characteristics											
IVSd (cm)	1±0.2	1.4±0.2	1.5±0.5	2.0±0.4	**<0.001**	**<0.001**	**<0.001**	1.00	0.62	1.00	**<0.001**
LVEDD (cm)	4.6±0.7	4.4±0.6	4.4±0.5	4.2±0.5	ns.	ns.	ns.	ns.	ns.	ns.	0.11
EF biplane (%)	63±4.4	61.1±6.8	61.5±9.5	62.1±8.7	ns.	ns.	ns.	ns.	ns.	ns.	0.82
GLS (%)	-20.5±2	-16.5± 2.3	-17.5±2.5	-16.1±3.7	**<0.001**	**0.006**	**<0.001**	1.00	1.00	1.00	**<0.001**
Peak E wave (m/s)	0.71±0.13	0.74±0.20	0.87±0.19	0.70±0.22	1.00	**0.02**	1.00	0.22	1.00	0.06	**0.02**
Peak A wave (m/s)	0.55±0.18	0.51±0.31	0.44±0.21	0.62±0.22	ns.	ns.	ns.	ns.	ns.	0.15	0.15
E/A	1.42±0.5	1.78±0.76	2.45±1.17	1.30±0.65	0.47	**<0.001**	1.00	0.05	0.36	**<0.001**	**<0.001**
E/E' average	6.5±1.5	7.8±2.8	9.9±3.4	8.7±3.3	0.46	**<0.001**	**0.03**	0.09	1.00	1.00	**<0.001**
TV Vmax (m/s)	2.0±0.5	2.1±0.6	2.5±0.3	2.4±0.4	1.00	**0.04**	0.33	0.35	1.00	1.00	**0.03**
DT (ms)	210±41.9	213.7±48.7	189.2±69.5	257.9±54	1.00	1.00	**0.01**	1.00	**0.06**	**0.003**	**0.003**
IVRT (ms)	71.9±19.3	88.1±26.1	87.2±44.4	107.3±25.2	0.21	0.51	**<0.001**	1.00	0.22	0.30	**<0.001**
SW measurements											
SWV(m/s)	3.4±1.0	4.3±1.3	6.5±1.1	8.7±1.2	0.06	**<0.001**	**<0.001**	**<0.001**	**<0.001**	**<0.001**	**<0.001**
Cardiac magnetic resonance measurements											
native T1 time (ms)	N/A	1000.±26	1047±17	1045±47	N/A	N/A	N/A	**<0.001**	**<0.001**	1.0	**<0.001**

post contr. T1 time (ms)	N/A	404.±36	419±54	381±54	N/A	N/A	N/A	ns.	ns.	ns.	0.11
ECV (%)	N/A	25±3	30±3	41±9	N/A	N/A	N/A	0.24	**<0.001**	**<0.001**	**<0.001**
T2 time (ms)	N/A	51±2	52±3	50±3	N/A	N/A	N/A	0.50	0.45	**0.03**	**0.04**

Values are mean ± SD, n/n (%), or median [IQR]. Abbreviations: A wave, late mitral valve inflow velocity; BMI, body mass index; BSA, body surface area; DBP, diastolic blood pressure; DT, deceleration time; E' average, average between septal and lateral mitral early relaxation velocity; E wave, early mitral valve inflow velocity; E/A, early to late mitral inflow velocity ratio; ECV, extracellular volume; E/E', mitral inflow to mitral relaxation velocity ratio; EF, ejection fraction; GLS, global longitudinal strain; HV = healthy volunteers; IQR, interquartile range; IVRT, isovolumetric relaxation time; IVSd, interventricular septum at end-diastole; LV, left ventricle; LVEDD, left ventricular end-diastolic dimension; MIF = myocardial interstitial fibrosis, MRF = myocardial replacement fibrosis; NF = no fibrosis; SD, standard deviation; SBP, systolic blood pressure; SWV = shear wave velocity; TV Vmax, maximal tricuspid regurgitation velocity.

Table 2: Linear regression analysis of predictors of myocardial fibrosis assessed with extracellular volume.

Independent variable	**Univariate regression**		**Multivariate regression**	
	r	p	beta	p
SWV	**0.70**	**<0.0001**	**0.72**	**<0.001**
age	0.17	0.30		
IVSD	**0.50**	**<0.001**		
LVEDD	-0.28	0.06		
E/E'	0.26	0.08		
TV Vmax	0.10	0.60		
DT	**0.32**	**0.04**		
IVRT	**0.35**	**0.03**		

Abbreviations: DT, deceleration time; E' average, average between septal and lateral mitral early relaxation velocity; E wave, early mitral valve inflow velocity; E/E', mitral inflow to mitral relaxation velocity ratio; IVRT, isovolumetric relaxation time; IVSd, interventricular septum at end-diastole; LV, left ventricle; LVEDD, left ventricular end-diastolic dimension; SWV, shear wave velocity; TV Vmax, maximal tricuspid regurgitation velocity.

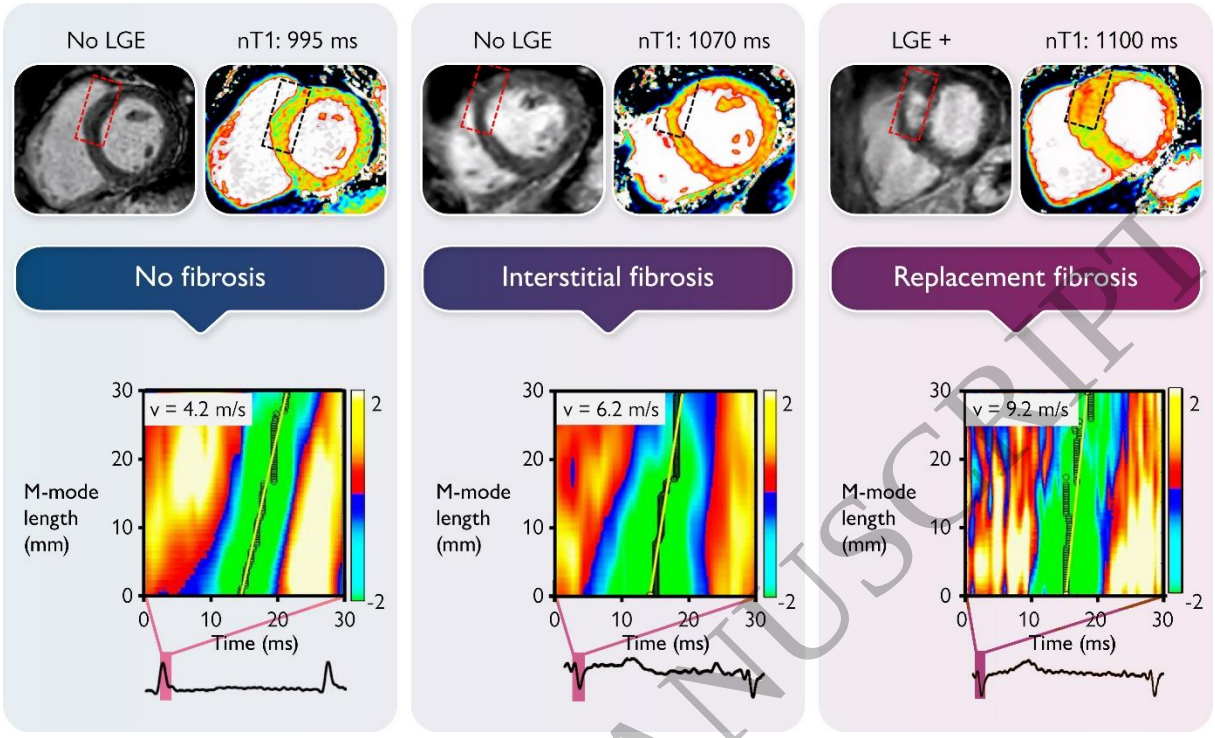

Figure 1
160x96 mm (DPI)

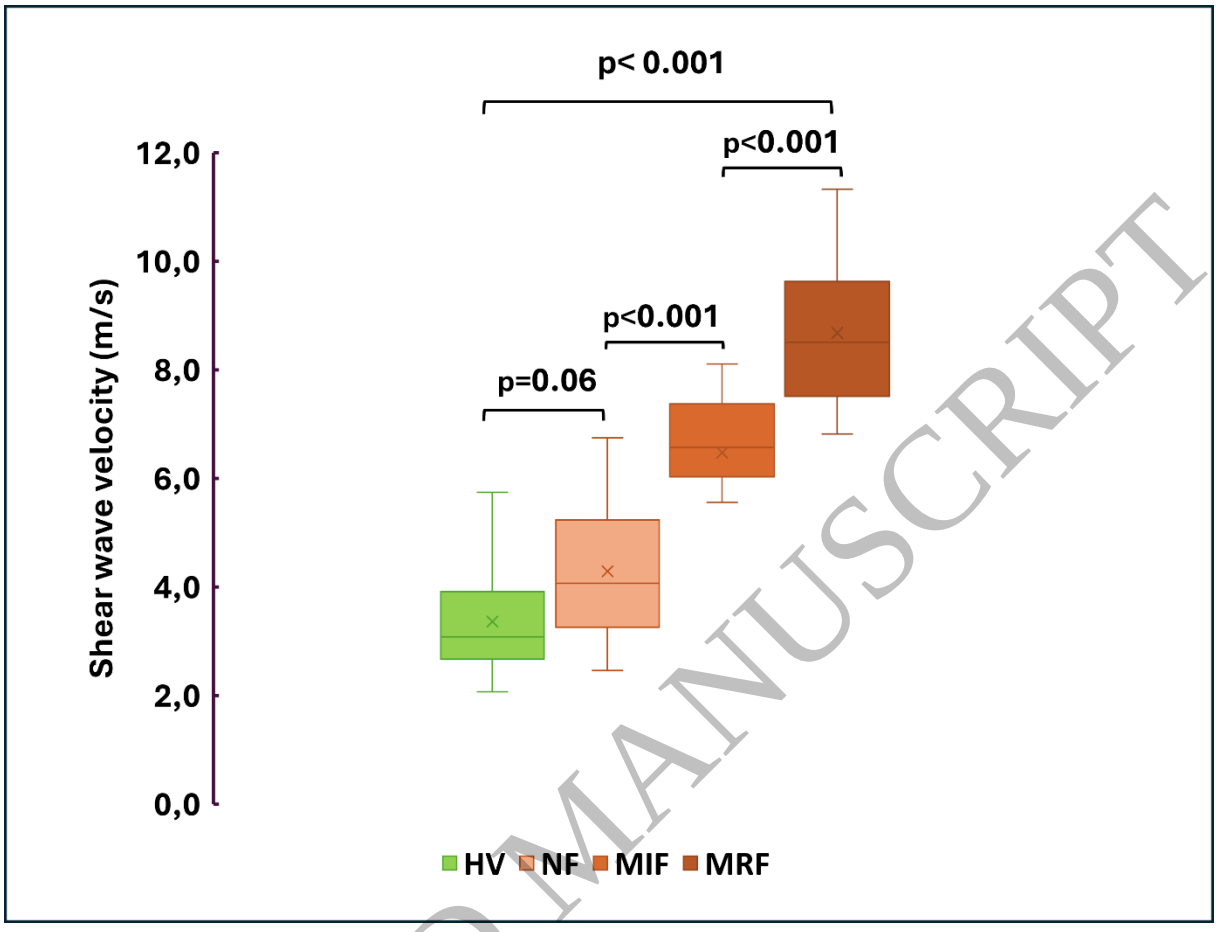

Figure 2
160x121 mm (DPI)

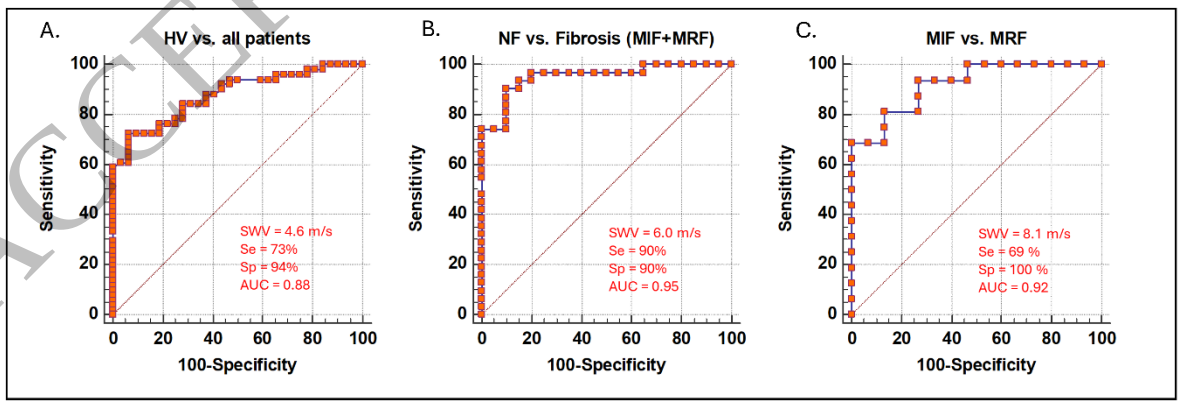

Figure 3
160x57 mm (DPI)

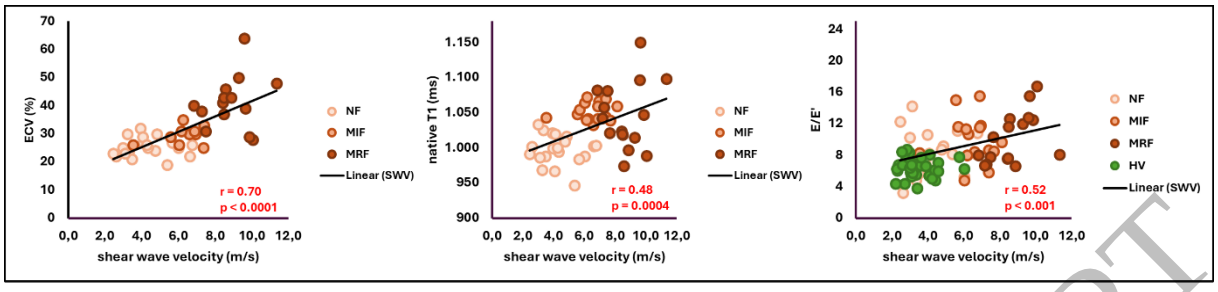

Figure 4
160x38 mm (DPI)

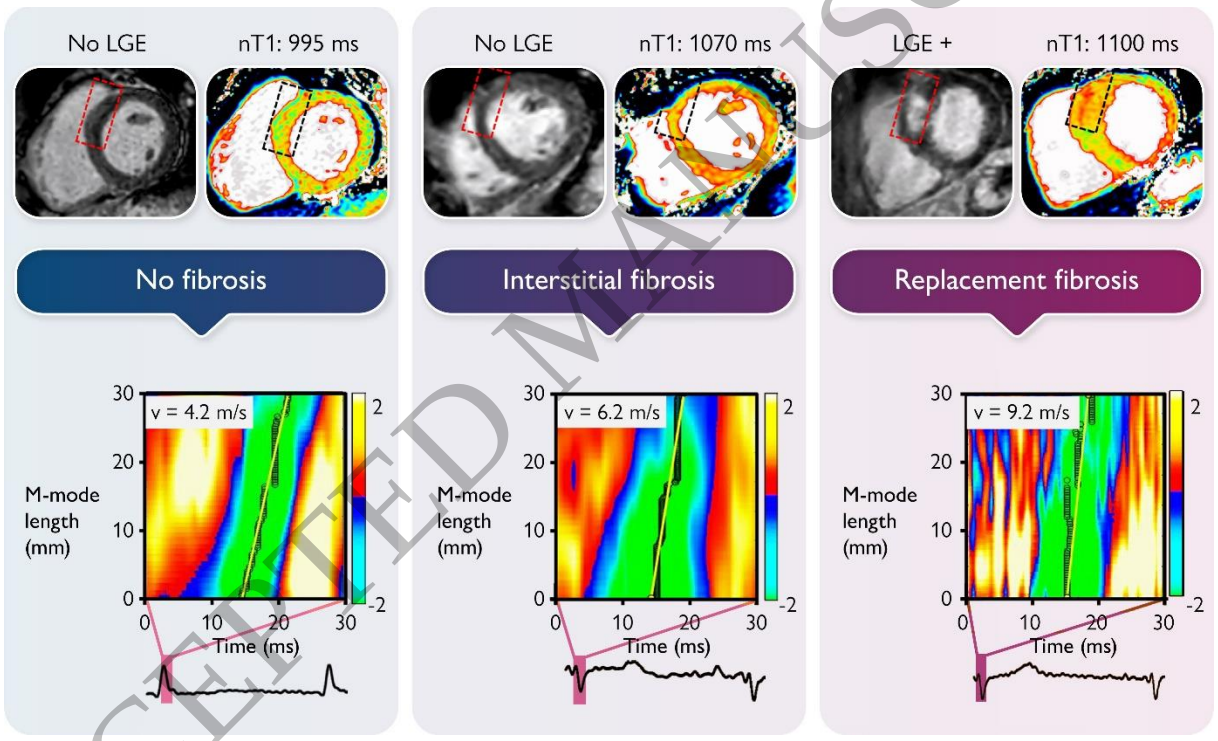

Graphical Abstract
160x96 mm (DPI)